Does Model Sensitivity to Changes in CO_2 Provide a Measure of Sensitivity to Other Forcings?

ANDREI P. SOKOLOV

Joint Program on the Science and Policy of Global Change, Massachusetts Institute of Technology, Cambridge, Massachusetts

(Manuscript received 25 April 2005, in final form 12 October 2005)

ABSTRACT

Simulation of both the climate of the twentieth century and a future climate change requires taking into account numerous forcings, while climate sensitivities of general circulation models are defined as the equilibrium surface warming due to a doubling of atmospheric CO_2 concentration. A number of simulations with the Massachusetts Institute of Technology (MIT) climate model of intermediate complexity with different forcings have been carried out to study to what extent sensitivity to changes in CO_2 concentration (S_{CO2}) represent sensitivities to other forcings.

The MIT model, similar to other models, shows a strong dependency of the simulated surface warming on the vertical structure of the imposed forcing. This dependency is a result of "semidirect" effects in the simulations with localized tropospheric heating. A method for estimating semidirect effects associated with different feedback mechanisms is presented. It is shown that forcing that includes these effects is a better measure of expected surface warming than a forcing that accounts for stratospheric adjustment only.

Simulations with the versions of the MIT model with different strengths of cloud feedback show that, for the range of sensitivities produced by existing GCMs, S_{CO2} provides a good measure of the model sensitivity to other forcings. In the case of strong cloud feedback, sensitivity to the increase in CO_2 concentration overestimates model sensitivity to both negative forcings, leading to the cooling of the surface and "black carbon"–like forcings with elevated heating. This is explained by the cloud feedback being less efficient in the case of increasing sea ice extent and snow cover or by the above-mentioned semidirect effects, which are absent in the CO_2 simulations, respectively.

1. Introduction

The Massachusetts Institute of Technology (MIT) 2D climate model has been used in a number of climate change–related studies in recent years. Forest et al. (2002) used the model to obtain a probability distribution for climate sensitivity consistent with the climate record for the twentieth century. This distribution was then used by Webster et al. (2003) for studying uncertainty in future climate change. In both cases, a number of different forcings were considered. For example, in simulations performed by Forest et al. (2002), the model was forced by changes in CO_2, sulfate aerosol, and ozone. In a more recent study (Forest et al. 2006), changes in solar constant, volcanic aerosol, and vegetation cover are also included. In projections of future climate, changes in different greenhouse gases, ozone, sulfate aerosol, and black carbon are taken into account. Climate sensitivities of different versions of the MIT climate model were, however, defined based exclusively on changes in CO_2 concentration. Therefore, it is important to evaluate to what extent model sensitivity to changes in CO_2 characterizes sensitivity to other forcings.

A number of climate change simulations with multiple forcings have been also performed recently with coupled atmosphere–ocean general circulation models (AOGCMs; Broccoli et al. 2003; Meehl et al. 2004; Stott et al. 2000).

The dependency of the climate system response to the external forcings on the nature of the forcing has been a subject of a number of recent studies (e.g., Cook and Highwood 2004; Feichter et al. 2004; Forster et al. 2000; Hansen et al. 1997, 2005; Penner et al. 2003; Ramaswamy and Chen 1997; Roberts and Jones 2004; Stuber et al. 2005). It was shown that the change in surface air temperature, ΔT_s, in response to changes in atmo-

Corresponding author address: Dr. Andrei Sokolov, Joint Program on the Science and Policy of Global Change, MIT E40-431, 77 Massachusetts Ave., Cambridge, MA 02139-4307.
E-mail: sokolov@mit.edu

spheric CO_2 concentration, solar constant, or surface albedo, and some others, is proportional to the adjusted radiative forcing at the tropopause, Fa, regardless of the nature of the forcing:

$$\Delta Ts = \lambda \mathrm{Fa}, \quad (1)$$

where λ is a climate sensitivity. This is not, however, the case for forcings due to changes in the concentration of ozone or absorbing aerosols (e.g., Hansen et al. 1997, 2005; Mickley et al. 2004; Roberts and Jones 2004; Stuber et al. 2005). Climate sensitivity to such forcings depends on their vertical structure. This dependency is explained by feedbacks related to the localized atmospheric heating caused by changes in ozone or absorbing aerosols. These feedbacks operate on shorter time scales than feedbacks associated with changes in surface temperature and are not excited by, for example, changes in CO_2 concentration.

Changes in radiation balance due to such fast feedbacks are often referred to as a "semidirect effect" (Hansen et al. 1997). It was shown that a forcing that includes semidirect effects is a better measure of climate sensitivity than an adjusted forcing that accounts for changes in stratosphere only.

A number of methods for estimating forcings that includes semidirect effects were proposed (Cook and Highwood 2004; Gregory et al. 2004; Hansen et al. 2005; Penner et al. 2003; Shine et al. 2003). Most of them were based on simulations with fixed surface or sea surface temperature. An alternative method based on the feedback calculations is proposed in this study. A somewhat similar approach was used by Stuber et al. (2005).

A number of the equilibrium climate change simulations with the versions of the MIT model with different climate sensitivities for a variety of forcings have been performed to study this issue. A brief description of the model is given in section 2. Dependence of model response on the vertical stratification of forcing and a method for calculating semidirect effects are discussed in section 3. In section 4 different ways of changing the sensitivity of the MIT models are described. Results of the simulations with the versions of the model with different sensitivities for different forcings are discussed in section 5. Conclusions are given in section 6.

2. Model description

The MIT 2D atmospheric model (Sokolov and Stone 1998) is a zonally averaged statistical–dynamical model developed from the Goddard Institute for Space Studies (GISS) general circulation model (GCM) Model II (Hansen et al. 1983). The model includes parameterizations of all the main atmospheric physical processes as well as parameterizations of heat, moisture, and momentum transports by eddy. The version used in this study has latitudinal resolution of 7.8° and nine vertical layers. Each cell can contain up to four different surface types: land, land ice, ice-free ocean, and ocean ice. The model calculates surface temperature, surface and radiative fluxes, and their derivatives with respect to surface temperature separately for different surface types.

A zonally averaged mixed layer model was used as the ocean component in the previous version of the MIT climate model. In the version used in this study, the atmospheric model is coupled to a mixed layer ocean model with a horizontal resolution 7.8° in latitude and 10° in longitude. Mixed layer depth is prescribed based on observations as a function of time and location.

The heat flux felt by the ocean model at the point (i, j) is calculated as

$$F_H(i,j) = F_{\mathrm{HZ}}(j) + \frac{\partial F_{\mathrm{HZ}}}{\partial T}(j)[Ts(i,j) - Tsz(j)],$$

where $F_{\mathrm{HZ}}(j)$ and $\partial F_{\mathrm{HZ}}/\partial T(j)$ are zonally averaged heat flux and its derivative with respect to surface temperature; $Ts(i, j)$ and $Tsz(j)$ are the surface temperature and its zonal mean, respectively.

The mixed layer model also uses a parameterized vertically averaged horizontal oceanic heat transport, the so-called Q flux. This flux has been calculated from a simulation in which sea surface temperature and sea ice distribution were relaxed to their present-day climatology.

As shown by Sokolov and Stone (1998), the MIT climate model simulates the zonally averaged features of the present-day atmospheric circulation reasonably well. Both equilibrium and transient responses to an increase in CO_2 concentration produced by the model are similar, in terms of global-average values and zonal distributions, to the responses obtained in simulations with 3D GCMs.

3. Model response to different forcings: Dependency on vertical structure of the forcing

A number of 150-yr-long equilibrium simulations with the MIT climate model with different forcing have been carried out (Table 1). During the last 20 yr, data required for radiation calculation have been saved and then used to calculate changes in radiation fluxes and climate feedbacks associated with changes in different climate variables (surface temperature, lapse rate, water vapor, cloud cover, and surface albedo). Feedbacks were calculated following the procedure proposed by Wetherald and Manabe (1988).

TABLE 1. Description of simulations.

Simulation	Type of forcing	Forcing at the tropopause (W m^{-2})	Forcing at the surface (W m^{-2})	Surface warming (K)	λ [K (W m^{-2})$^{-1}$]
2×CO2	Doubled CO_2 concentration	3.76	0.8	2.18	0.58
0.5×CO2	Halved CO_2 concentration	−3.76	−0.56	−2.14	0.57
2%S0	2% increase in solar constant	4.72	3.56	2.28	0.48
−2%S0	2% decrease in solar constant	−4.72	−3.56	−2.22	0.47
ALB	Increase in surface albedo	−3.39	−3.85	−1.54	0.45
STRAER	Increase in stratospheric aerosol concentration	−3.92	−4.08	−1.87	0.48
10BC	Change in black carbon simulated by the MIT climate-chemistry model multiplied by 10	2.36	−4.44	1.76	0.75
LWBC	Fixed longwave forcing with vertical structure of the global- and annual-mean black carbon forcing	2.36	−4.44	1.76	0.74
LWBCL3	Fixed longwave forcing with the same changes at the TOA and at the surface as in LWBC, but with the absorbing layer shifted to 800 hPa	2.36	−4.44	1.23	0.52
LWBCL6	Fixed longwave forcing with the same changes at the TOA and at the surface as in LWBC, but with the absorbing layer shifted to 320 hPa	2.36	−4.44	0.64	0.27

Climate feedbacks produced by the model are used in comparison of the model responses to different forcings shown below. It is, therefore, important to know how the MIT model compares with other models in this respect. Figure 1 shows strengths of climate feedbacks in equilibrium doubled CO_2 simulations with a number of GCMs. The circles indicated feedbacks from an analogous simulation with the MIT 2D model. Data for different GCMs are taken from Colman (2003). As can be seen, all feedbacks produced by the MIT model fall in the range shown by GCMs. However, both cloud feedback and the total feedback are rather weak.

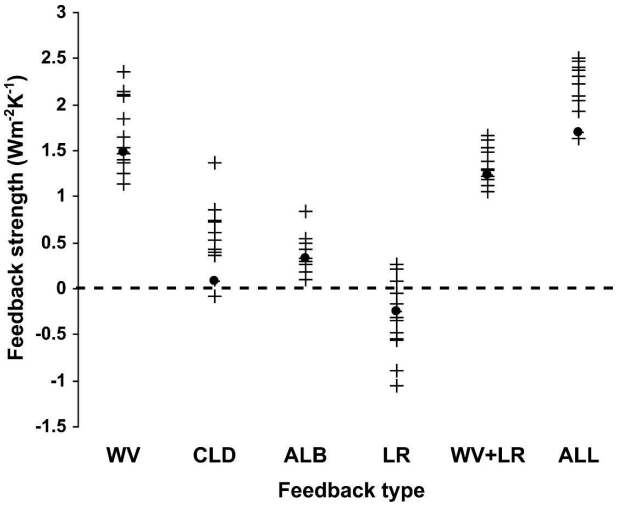

FIG. 1. Strengths of feedbacks (W m^{-2} K^{-1}) in doubled CO_2 simulations with different GCMs (+) and with the MIT climate model (circles). Data for GCMs are from Colman (2003).

The feedbacks shown in Fig. 1 and later in the paper are calculated as changes in the radiation balance (positive downward) at the tropopause associated with changes in a particular climate variable, such as clouds or water vapor, divided by the change in surface air temperature caused by the particular forcing.

To evaluate model response to changes in black carbon (BC) concentration an equilibrium climate change simulation (10BC) has been carried out, using changes in black carbon loading simulated by the MIT climate-chemistry model (Wang et al. 1998). Projected changes in BC are small, and so are forcings associated with these changes. To obtain a statistically significant response changes in BC loading were multiplied by 10. Such an increase in BC yields a positive forcing of 2.4 W m^{-2} at the tropopause and a strong negative forcing of −4 W m^{-2} at the surface (Fig. 2a). In spite of such a strong cooling at the surface, surface temperature actually increases by 1.76° in this simulation. This is explained by the vertical distribution of the BC forcing.

As was shown by Hansen et al. (1997), effectiveness of forcing with respect to surface warming depends on the altitude at which forcing is applied. They carried out simulations applying forcing of 4 W m^{-2} at each layer of the model and at the surface. Results of those simulations are shown in Fig. 3 together with the results of analogous simulations with the MIT 2D model. Both models show a similar dependency of the model response on the altitude of the forcing, but the GISS model is noticeably more sensitive to the forcings applied in the low troposphere and at the surface. The two top layers (8 and 9) and a part of layer 7 are located in

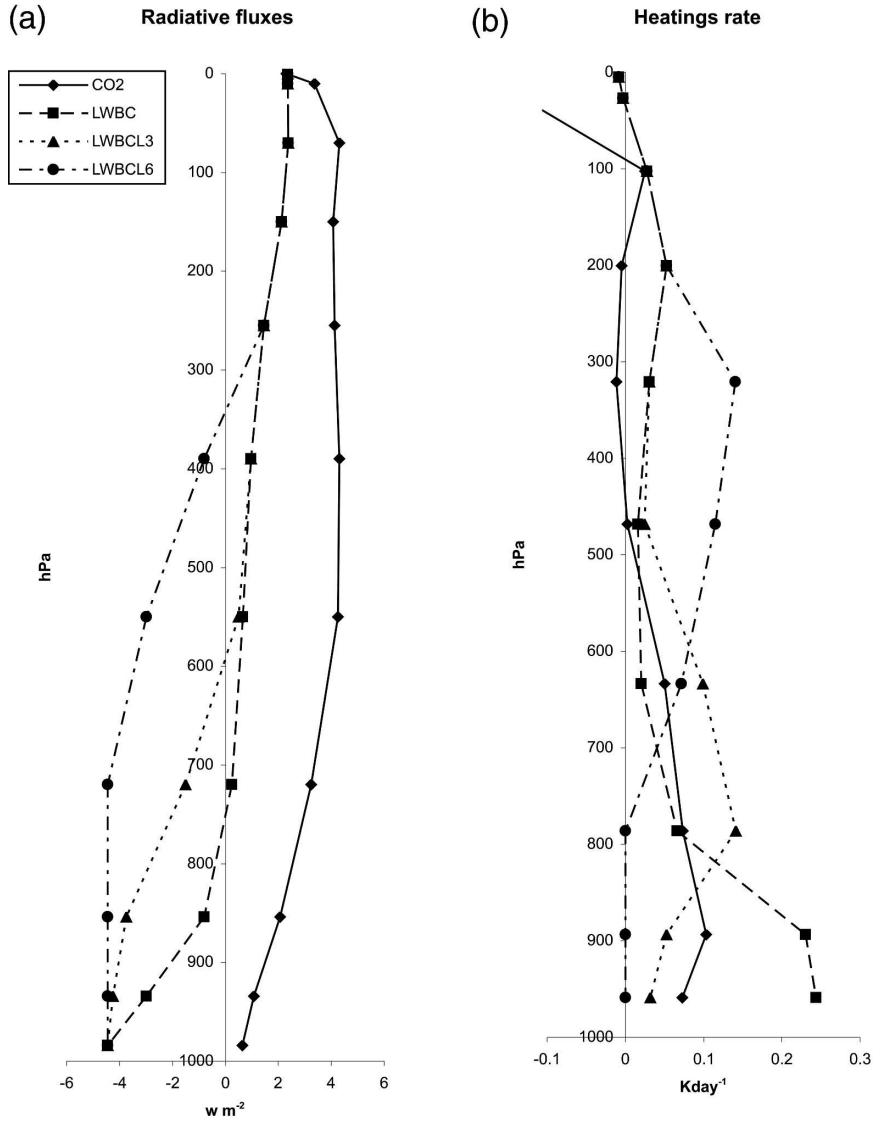

FIG. 2. Vertical distribution of radiative fluxes (W m^{-2}) and heating rates (K day^{-1}) due to doubling of CO_2 and due to BC-like forcings.

the stratosphere and, as indicated by Hansen et al. (1997), when the forcing is applied in those layers an adjusted forcing on the tropopause is significantly smaller than the applied forcing. Therefore, only results for simulations with forcings in the six low layers are discussed below. The two feedbacks that show the largest differences (Table 2) are lapse rate feedback and cloud feedback. The lapse rate feedback is negative in all simulations. It is weakest for the forcing in layer 2 and becomes much stronger when the forcing is applied in the top layers. These differences to a large extent are offset by changes in the water vapor feedback, but the sum of these two feedbacks is still 30% larger for the forcing in the second layer than for the forcing in layer 6. The cloud feedback is positive when forcing is applied in the two lowest layers and also becomes strongly negative when forcing is applied in the top layers.

Cloud cover decreases in all simulations. Changes in clouds affect longwave and shortwave radiative fluxes at the top of the atmosphere (TOA) in opposite directions. Such decrease in cloud cover reduces planetary albedo and leads to the increase in the shortwave radiation absorbed by earth. On the other hand, since clouds emit longwave radiation at the lower temperature than the surface, decrease in clouds will result in the increase in outgoing longwave radiation (OLR). Change in the net radiative balance at the TOA depends on the relative magnitudes of changes in the

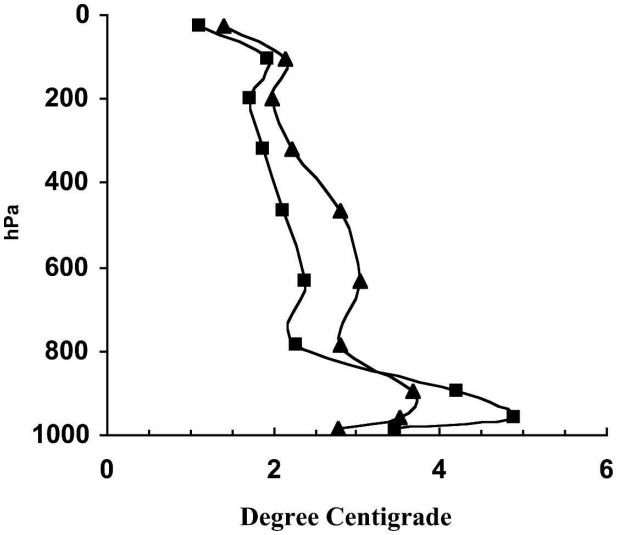

FIG. 3. Dependence of surface air temperature increase on the altitude at which forcing was applied. Triangles: the MIT 2D model; squares: the GISS AGCM.

shortwave and longwave components. Decrease in high clouds due to their relatively small albedo and large difference between temperature of the cloud top and surface temperature will mainly affect OLR leading to the decrease in the net radiative flux at the TOA and to the negative cloud feedback. Decrease in low clouds, which have a larger albedo and a temperature not much different from temperature of the surface will, in contrast, lead to a positive cloud feedback.

In simulations with the MIT model high clouds decrease in response to surface warming. Warming of a particular model layer causes an additional decrease in cloud cover in that layer. Cloud feedback associated with localized tropospheric warming may be either negative or positive and will enhance or offset negative cloud feedback associated with surface warming, respectively.

As a result, changes in radiative fluxes in all simulations, except the one with forcing applied directly to surface, consist of two components: one related to the tropospheric warming (semidirect effects), F_{SMD}, and another caused by surface warming, H_{SRF}. Those components can be separated from each other in a number of ways, for example, by performing parallel simulations with fixed surface temperature (Cook and Highwood 2004; Hansen et al. 2005; Penner et al. 2003; Shine et al. 2003). It also can be done assuming that changes caused by warming of a particular atmospheric layer and changes caused by surface warming are additive and that the latter are proportional to surface temperature increase. Under the second assumption, change in radiative flux related to the surface warming in the simulation with forcing applied in the layer L can be calculated as $H^L_{\mathrm{SRF}} = H^0/\Delta T^0 \cdot \Delta T^L$, where H^0 is change in a radiation flux in simulation with forcing applied at the surface, and ΔT^0 and ΔT^L are changes in surface air temperature in two simulations. Then change in flux due to semidirect effect (semidirect forcing) is

$$F^L_{\mathrm{SMD}} = H^L - \frac{H^0}{\Delta T^0}\Delta T^L, \tag{2}$$

where H^L is a total change in a radiative flux in simulation with forcing applied at a layer L.

Using Eq. (2), semidirect forcings associated with changes in different climate variable can be calculated from feedbacks (Table 2). Semidirect forcings due to changes in lapse rate and water vapor (together) and clouds are shown in Table 3. As could be expected from Fig. 2, semidirect effect is significant for forcings applied in the planetary boundary layer and upper troposphere and is mainly related to changes in clouds. The "corrected" forcing (Fc) is calculated as a sum of adjusted and total semidirect forcings, and λc is a model sensitivity calculated from Eq. (1), using Fc instead of Fa. As can be seen, λc shows practically no dependency on location of the forcing and is very close to values obtained in simulations with changes in CO_2, solar constant, or stratospheric aerosol.

Change in radiative fluxes caused by an increase in the loading of BC leads to the warming concentrated in the two lowest model layers (Fig. 2b) with a maximum

TABLE 2. Strengths of different feedbacks (W m^{-2} K^{-1}) in simulations with 4 W m^{-2} forcing applied at different heights (LR: lapse rate; Q: water vapor; CLD: clouds; ALB: surface albedo).

L	Height (hPa)	LR	Q	LR+Q	CLD	ALB	LR+Q+CLD+A
0	984	−0.342 29	1.503 29	1.161 00	−0.131 43	0.352 04	1.381 61
1	958	−0.275 86	1.480 09	1.204 23	0.232 15	0.305 44	1.741 83
2	894	−0.144 1	1.445 07	1.300 26	0.370 37	0.289 29	1.959 93
3	786	−0.291 61	1.489 04	1.197 43	−0.082 82	0.329 35	1.443 97
4	633	−0.422 74	1.558 14	1.135 40	−0.140 18	0.338 24	1.333 46
5	468	−0.616 40	1.704 13	1.087 73	−0.282 29	0.345 65	1.151 09
6	320	−0.976 63	2.007 95	1.031 32	−0.725 12	0.375 52	0.681 72

TABLE 3. Changes in surface air temperature ΔTs (K), radiative fluxes at the tropopause due to changes in lapse rate and water vapor (together) and clouds H_{LR+Q} and H_{CLD}, their fractions not related to surface warming F_{LR+Q} and F_{CLD}, semidirect and corrected forcings F_{SMD} and Fc, and sensitivity parameter λc corresponding to Fc.

L	ΔTs (K)	H_{LR+Q} (W m^{-2})	H_{CLD} (W m^{-2})	F_{LR+Q} (W m^{-2})	F_{CLD} (W m^{-2})	F_{SMD} (W m^{-2})	Fc (W m^{-2})	λc K (W m^{-2})$^{-1}$
0	2.08	2.265 84	−0.3253	0	0	0	4	0.52
1	2.77	3.113 89	0.589 23	0.0964	1.022 44	1.118 84	5.118 84	0.54
2	3.02	3.676 66	1.046 52	0.386 83	1.518 83	1.905 67	5.905 67	0.51
3	2.24	2.526 65	−0.270 84	0.086 51	0.079 48	0.166	4.166	0.54
4	2.02	2.162 39	−0.357 92	−0.038 09	−0.042	−0.080 09	3.919 91	0.52
5	1.92	2.011 08	−0.637 41	−0.080 46	−0.337 13	−0.4176	3.5824	0.54
6	1.55	1.598 97	−1.233 55	−0.089 52	−0.991 14	−1.080 66	2.919 34	0.53

around 950 hPa. This warming causes a positive feedback that is strong enough to overcome direct cooling at the surface. As shown by Hansen et al. (1997, 2005) and Cook and Highwood (2004), climate impact of the increase in BC concentration strongly depends on vertical distribution of black carbon.

To evaluate the dependency of the MIT model response to the vertical stratification of the "BC like" forcing, three simulations with longwave forcing have been carried out. In the first simulation (LWBC), LW forcing with the same vertical distribution as an annual-mean global-mean forcing due to changes in BC has been used. Despite differences in the nature as well as in spatial and temporal patterns of the forcing between 10BC and LWBC, global-mean annual responses are very similar in these simulations. Forcings applied in the other two BC-like simulations (LWBCL3 and LWBCL6) have the same change at the tropopause and at the surface, but the "absorbing layer" is shifted up (Fig. 2). As a result maximum change in the heating is concentrated at about 800 and 320 hPa. These forcings lead to a noticeably smaller surface warming, namely, 1.23 and 0.64 K instead of 1.76 K.

Decrease in low clouds in LWBC simulation (Fig. 4a), while smaller in magnitude than the decrease in high clouds, is nevertheless strong enough to produce positive cloud feedback (Table 4). Air temperature change (Fig. 4b) in the LWBC simulation, while smaller than in the simulation with forcing applied directly at the surface (SRF), has a similar shape throughout most of the troposphere. In the other two simulations, especially in the LWBCL6 simulation, the warming increases faster with height. Differences in the vertical structure of the forcing also affect changes in the hydrological cycle. Changes in both relative humidity and heating due to moist convection show a strong dependence on vertical structure of the forcing (Fig. 5). Those differences are reflected in the strengths of different feedbacks (Table 4). Such strong negative lapse rate and cloud feedbacks in a simulation with the forcing concentrated in the upper troposphere lead to the total feedback being negative.

Semidirect forcings in the last three simulations are shown in Table 5. As can be seen in the table, if the components of the cloud feedback and the combined lapse rate and water vapor feedbacks that are not related to surface warming are treated as forcing, Eq. (1) provides a good estimate of model sensitivity.

The "corrected" forcing defined above accounts for both stratospheric and tropospheric adjustment and, in this way, is similar to forcings defined in a number of studies, such as "adjusted troposphere and stratosphere forcing" by Shine at al. (2003) or Fs forcing of Hansen et al. (2005).

If heating is located in the low troposphere Fc is larger than Fa, but becomes smaller when the "absorbing layer" is shifted upward. Overall, similar dependency was found by Hansen et al. (2005) between Fs and Fa in simulations with changes in BC in individual layers (their Table 2 and Fig. 27a). To compare different methods, simulations with fixed sea surface temperature and sea ice distributions were carried out for LWBC, LWBCL3, and LWBCL6 forcing; Fs forcing was then calculated from Eq. (1) of Hansen et al. (2005), using a climate sensitivity parameter (λ) from the SRF simulation. Hansen et al. (2005) used a sensitivity parameter evaluated from the simulation with doubled CO_2. For the MIT model, Fc seems to be a better estimate for expected surface warming than Fs; λc is closer to the sensitivity parameter estimated from the SRF simulation than λs.

4. Changing sensitivity of the MIT model

The sensitivity of the MIT climate model is varied by changing the strength of the cloud feedback (Sokolov and Stone 1998). Namely, the cloud fractions used in the radiation calculation are calculated as

$$C = C^0 (1.0 + k\Delta T_{srf}), \quad (3)$$

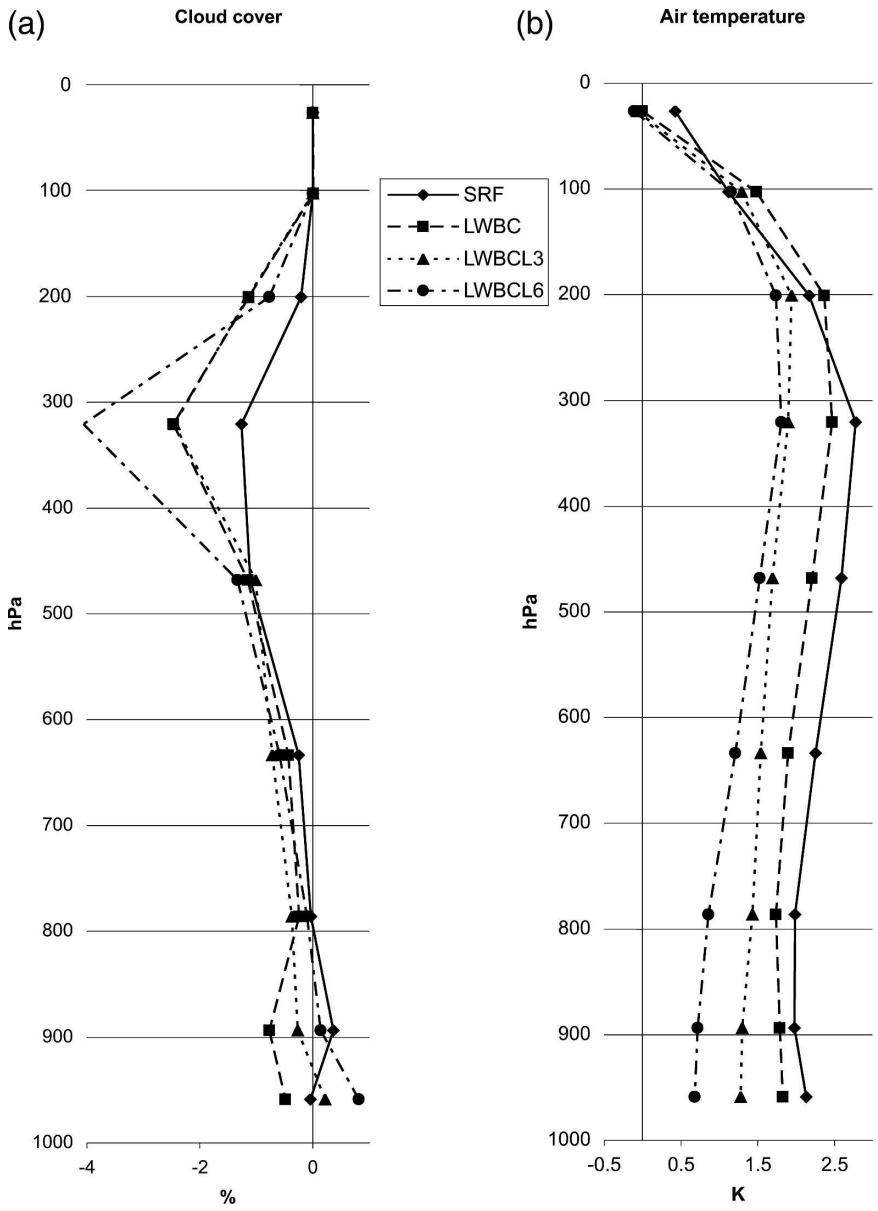

FIG. 4. Changes in clouds (%) and air temperature (K) in simulations with surface and BC-like forcings.

where C^0 is cloud cover calculated by the model and ΔT_{srf} is the difference of global-mean surface air temperature from its value in a control climate simulation. By changing the parameter k, different sensitivities are obtained. For example, with k equal to 0.04 and -0.03, the sensitivities to the CO_2 doubling are 1.4 and 4.1 K, respectively. The natural sensitivity of the model ($k = 0$) is 2.2 K.

TABLE 4. Strengths of different feedbacks (W m^{-2} K^{-1}) in simulations with black carbon–like forcings.

Forcing	LR	Q	LR+Q	CLD	ALB	LR+Q+CLD+A
LWBC	−0.405	1.630	1.225	0.361	0.269	1.855
LWBCL3	−0.719	1.789	1.070	−0.134	0.294	1.230
LWBCL6	−2.253	1.827	0.574	−1.254	0.325	−0.356

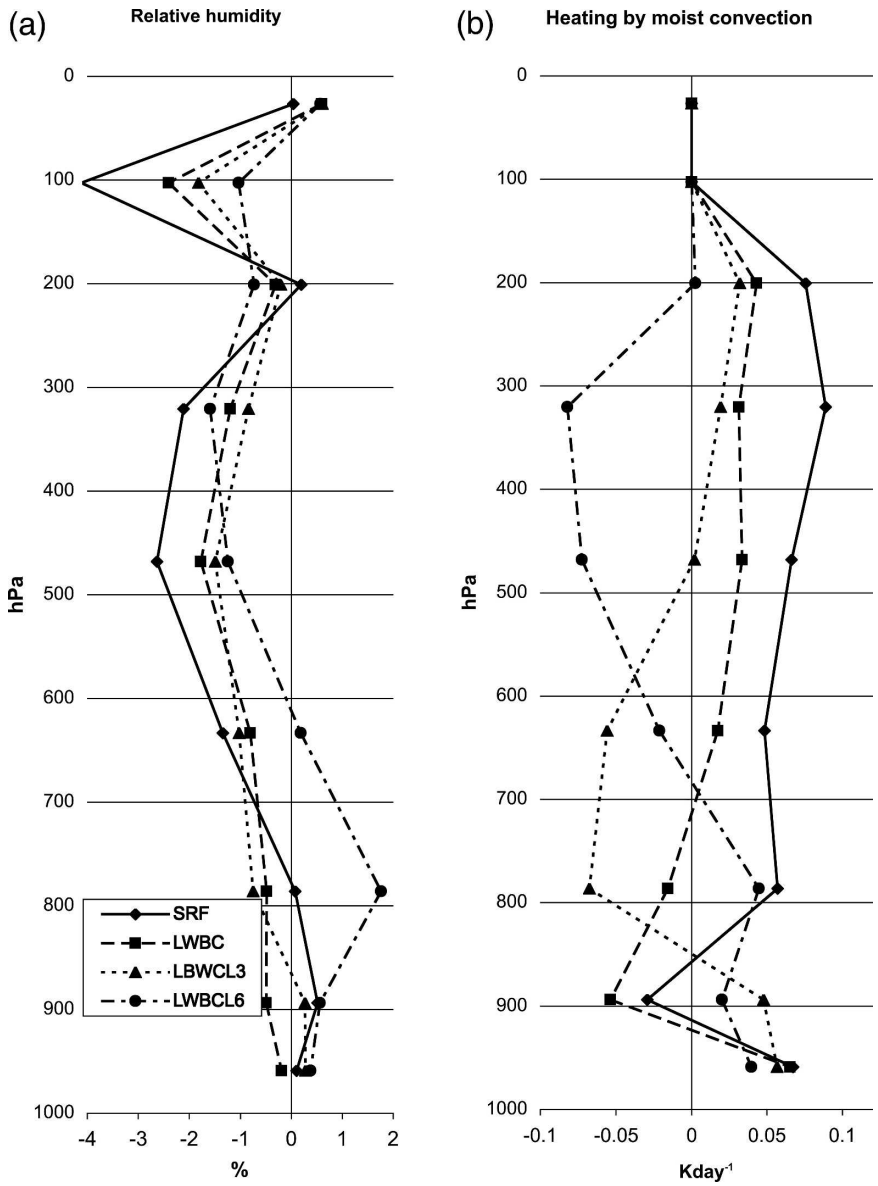

FIG. 5. Same as in Fig. 4 but for relative humidity (%) and heating rate (K day^{-1}) due to moist convection.

Use of Eq. (3), however, leads to the simultaneous increase/decrease in both high and low clouds, which, as mentioned above, has effects of opposite sign on climate sensitivity. Such as, if Eq. (3) with $k = -0.03$ is applied to low and middle clouds, only model sensitivity increases up to 5.0 K. On the other hand, if only high clouds are changed, then sensitivity decreases to 1.9 K. And finally, if $k = -0.03$ is used for low and middle

TABLE 5. Semidirect forcings associated with changes in lapse rate and water vapor (together) and clouds F_{LR+Q} and F_{CLD}, total semidirect and corrected forcings F_{SMD} and Fc, Fs forcing as defined by Hansen et al. (2005), and sensitivity parameters λc and λs corresponding to Fc and Fs, respectively, for simulations LWBC, LWBCL3, and LWBCL6.

Forcing	ΔTs (K)	F_{LR+Q} (W m^{-2})	F_{CLD} (W m^{-2})	F_{SMD} (W m^{-2})	Fc (W m^{-2})	λc [K (W m^{-2})$^{-1}$]	Fs (W m^{-2})	λs [K (W m^{-2})$^{-1}$]
LWBC	1.78	0.551 81	0.912 128	1.463 938	3.833 938	0.464 275	4.571 399	0.408 965
LWBCL3	1.23	0.405 662	−0.025	0.380 658	2.750 658	0.447 166	3.187 757	0.412 638
LWBCL6	0.71	0.219 856	−0.887 08	−0.667 22	1.702 776	0.416 966	2.276 214	0.319 417

clouds and $k = 0.03$ for high clouds, sensitivity of the model becomes 6.9 K.

Changing high and low clouds in opposite directions allows one to obtain the same sensitivity with a smaller value of k compared to using the same value of k for all clouds. It decreases artificial changes in cloud cover in simulations with different sensitivities.

Figure 6 shows a comparison of the results from the doubled CO_2 equilibrium simulations with the versions of the MIT model with different sensitivities with the results obtained in similar simulations with different GCMs (Feichter et al. 2004; Meleshko et al. 2000; Murphy et al. 2004; Senior and Mitchell 1993; Washington and Meehl 1993; Yao and Del Genio 1999). Results from the simulations in which sensitivity of the MIT model was changed using the same value of parameter k for all clouds are shown by diamonds. Triangles indicate result from the simulations in which k of opposite signs were used for high and low clouds. Results of GCMs are shown by squares. Overall, the latter way of varying sensitivity of the MIT model produces better agreement with GCMs and was used in the simulation discussed below. Some of the GCMs used for comparison are fairly old. However, as was shown by Cubash et al. (2001), dependency of the changes in global precipitation, and therefore evaporation, on surface warming produced by the models used in Third Assessment Report is similar to the dependency shown by the models used in the Second Assessment Report. The same is likely to be true for other components of a surface heat balance.

Strengths of different feedbacks for four versions of the MIT model are shown in Table 6. Not surprisingly, changes in sensitivity are mainly associated with differences in cloud feedback. Changes in the lapse rate feedback to a large extent are compensated by changes in the water vapor feedback. Such compensation between lapse rate and water vapor feedbacks in the doubled CO_2 simulations is a feature shown by practically all models (see Colman 2003).

5. Model sensitivity to CO_2 increase as a measure of model sensitivity to other forcings

Published results of the simulations with different GCMs do not provide a definitive answer to whether models' sensitivities to increase in CO_2 concentration (S_{CO2}) reflect sensitivities to other forcings. Models' responses to changes in solar constant and surface albedo are in general consistent with their sensitivities to changes in CO_2 concentration. Comparison of simulations with changes in black carbon or ozone is complicated by differences in simulations design. Both Hansen et al. (1997) and Cook and Highwood (2004) performed simulations with changes in black carbon; however, magnitudes and vertical structures of those changes were different. Joshi et al. (2003) compared responses of three GCMs—University of Reading (UREAD), ECHAM4, and Laboratoire de Météorology Dynamique (LMD)—to an increase in CO_2 concentration, solar constant, and upper-tropospheric ozone. Magnitudes of changes were chosen so as to produce a forcing of 1 W m^{-2} in all cases. For all three forcings, the strongest response was produce by LMD and the weakest by the UREAD model. Differences in sensitivity between models, however, depend on forcing. Ratios of surface warming simulated by UREAD and LMD models to that simulated by ECHAM4 for different forcing are shown in Table 7. The ratio of sensitivities to ozone is smaller than the ratio of sensitivities to CO_2 for the UREAD model while it is larger for the LMD model. Overall, however, ratios for a given model differ by less than 20%.

To see how well sensitivities of the different versions of the MIT model to the CO_2 doubling reflect their sensitivities to other forcings, five additional simulations with different values of k [see Eq. (3)] have been carried out for each forcing. Sensitivities to the doublings of CO_2 concentration corresponding to the chosen values of k are shown in the first rows of Tables 8 and 9. Table 8 also shows ratios of the surface air temperature (SAT) changes in those simulations to the SAT change in the simulation with a standard sensitivity ($k = 0$) for each forcing. SAT changes in the simulations with $k = 0$ are given in Table 1.

Sensitivity to CO_2 forcing serves as a good measure for sensitivities to the 2% S0 and SRF forcings but noticeably overestimates sensitivities to forcings causing a decrease in surface temperature (−2% S0, 0.5×CO2, ALB, and STRAER; see Table 1). The ratio of the SAT changes in the STRAER simulation with $S_{CO2} = 7.45$ K is about half as large as in corresponding 2×CO2 simulation. High sensitivities to changes in CO_2 concentration are primarily caused by large positive shortwave cloud feedback. Significant increase in sea ice and snow cover in the last four simulations decreases the effect of changes in cloud on shortwave radiation and therefore decreases efficiency on an additional cloud feedback. As a result the range of sensitivities to such forcing is narrower than the range of sensitivities to changes in CO_2 concentration.

Since differences in sensitivities between different versions of the MIT climate model are entirely due to differences in cloud feedback the MIT model will exaggerate the difference in sensitivities to positive and

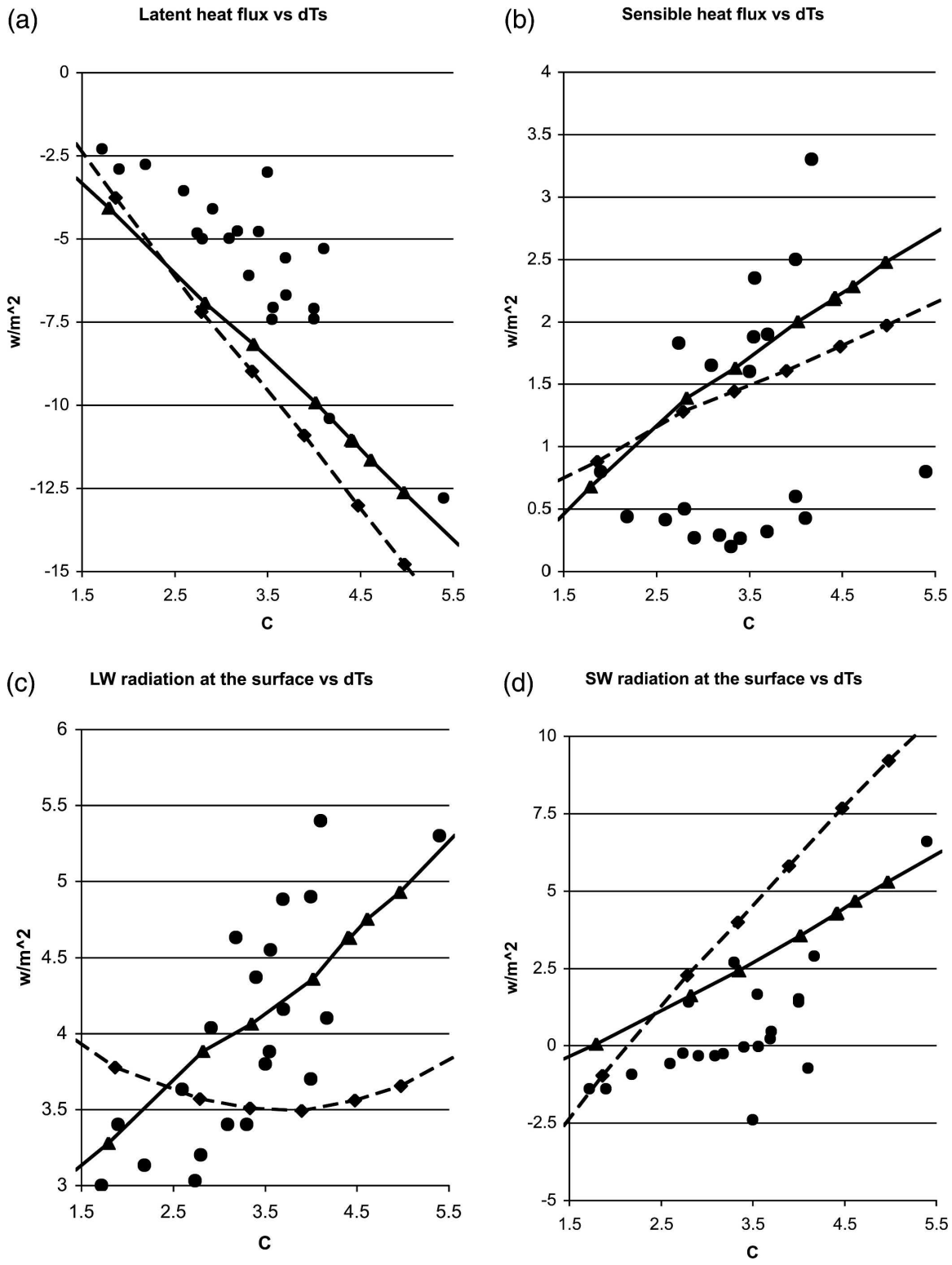

FIG. 6. Changes in surface fluxes (W m^{-2}) in equilibrium doubled CO_2 simulations with different GCMs (circles) and the versions of the MIT climate model with different sensitivities. Diamonds indicate results from the versions with the same *k* used for all clouds, and triangles indicate results from the simulations with k of different signs used for high and low clouds.

TABLE 6. Feedbacks (W m^{-2} K^{-1}) in doubled CO_2 simulations with different climate sensitivities.

ΔTs (K)	LR	Q	LR+Q	CLD	ALB
1.39	−0.052	1.365	1.313	−1.030	0.334
2.18	−0.195	1.488	1.293	0.068	0.258
4.50	−0.289	1.577	1.288	0.959	0.241
7.45	−0.308	1.633	1.325	1.208	0.311

TABLE 7. Ratios of SAT changes in the simulations with UREAD and LMD GCMs to that in the simulations with ECHAM4.

Forcing	UREAD/ECH	LMD/ECH
CO_2	0.47	1.38
S0	0.38	1.30
O_3	0.41	1.62

negative forcing.[1] At the same time differences in the strengths of cloud feedbacks also account for a large part of the differences in climate sensitivities between different GCMs (Cess at al. 1990; Colman 2003), and above-discussed interaction between cloud and surface albedo might be relevant for other models.

As shown in section 3, changes in the radiation fluxes associated with changes in different climate variables and, therefore, strengths of different feedbacks in BC-like simulations only partially relates to the surface warming and partially to the warming at the height of the absorbing layer. The component of feedbacks not related to surface warming is rather close in magnitude in the simulations with different S_{CO2} (Table 9) making the range of the model's sensitivity to BC-like forcings smaller than for CO_2 forcing. Model sensitivities calculated from Eq. (1) using "corrected" forcing are again close to sensitivities in corresponding simulations with CO_2 or direct surface forcings.

6. Conclusions

Simulations with the MIT climate model are shown to be similar to the findings of previous studies (e.g., Cook and Highwood 2004; Hansen et al. 1997, 2005; Mickley et al. 2004; Roberts and Jones 2004)—a strong dependence of the model response on vertical structure of the imposed forcing. Heating in the lowest 1500 m produces much stronger surface warming than an equivalent heating of the upper layers. Such dependency of surface warming on the altitude of heating is explained by the cloud and joint water vapor/lapse rate feedbacks not related to the surface warming. If, however, changes in radiation fluxes associated with the tropospheric warming are treated as a semidirect forcing, then the total forcing provides a good measure for the increase in surface temperature. Forcing defined in such a way accounts for both tropospheric and stratospheric adjustment and, in this sense, is similar to a number of forcings proposed in previous studies (e.g., Cook and Highwood 2004; Gregory et al. 2004; Hansen et al. 2005; Penner et al. 2003; Shine et al. 2003; Stuber et al. 2005).

Simulations with versions of the MIT model with different strengths of cloud feedback show that model sensitivity to the increase in CO_2 concentration reasonably well characterizes the model's sensitivity to other positive forcing with similar vertical structure. In the case of the forcings leading to surface cooling, an increase in the strength of cloud feedback is less efficient due to an increase in sea ice extent and snow cover and associated with that increase in surface albedo. Since differences in cloud feedback are one of the main reasons for the differences in sensitivities between different GCMs, this implies that the range of the models' responses to such forcing as an increase in stratospheric aerosol or decrease in solar constant might be narrower than the range of responses to a CO_2 increase.

Sensitivity to changes in the CO_2 concentration is defined by strengths of climate feedbacks related to surface warming. A distinguishing feature of the simulations with black carbon–like forcings is a presence of additional feedbacks related to the warming at the lo-

TABLE 8. Ratios of SAT changes in the simulations with low and high sensitivities to that in the simulations with standard sensitivity.

S_{CO2} forcing	0.48	1.39	4.50	5.62	7.45
2×CO2	0.22	0.63	2.06	2.58	3.42
SRF	0.22	0.61	1.93	2.60	3.29
2%S0	0.21	0.6	1.96	2.39	3.39
−2%S0	0.20	0.59	1.53	1.69	1.83
0.5×CO2	0.19	0.59	1.41	1.69	1.82
ALB	0.20	0.59	1.44	1.56	1.82
STRAER	0.16	0.51	1.41	1.52	1.65
10BC	0.19	0.61	1.81	2.15	2.40
LW_BC	0.22	0.61	1.80	2.13	2.47
LW_BC_L3	0.20	0.60	1.74	2.08	2.46
LW_BC_L6	0.21	0.63	2.05	2.40	2.85

[1] As a result the MIT model might underestimate impacts of decrease in solar constant or increase in stratospheric aerosol due to volcanic eruptions. It should be kept in mind that forcings used in the above-described simulations (see Table 1) are much stronger than the observed ones. For the weaker forcings, this effect will much weaker.

TABLE 9. Ratios of "corrected" forcings in the BC-like simulations with low and high sensitivities to that in the simulations with standard sensitivity.

S_{CO2} forcing	0.48	1.39	4.50	5.62	7.45
LWBC	1.01	0.98	0.89	0.82	0.75
LWCBL3	0.8	1	0.87	0.79	0.75
LWBCL6	0.77	0.77	0.92	0.89	0.79

cation of the absorbing layer (semidirect forcing). Therefore, sensitivities defined through doubled CO_2 simulations may not provide good estimates for the sensitivities to forcing with different vertical structures. Thus, the range of the MIT model responses to changes in black carbon concentration and black carbon–like forcings is also smaller than that to changes in CO_2. The latter is explained by semidirect forcings having similar magnitude in the simulations with different strengths of cloud feedback. Large differences, however, occur for values of S_{CO2} outside of the range produced by existing GCMs.

Acknowledgments. I would like to thank Chris Forest and Peter Stone, as well as Piers Forster and an anonymous reviewer for useful comments, which led to an improvement of the paper; Rob Colman for providing data on the feedbacks in different GCMs used in Fig. 1; and colleagues from different institutions for data used in Fig. 6.

REFERENCES

Broccoli, A. J., K. W. Dixon, T. L. Delworth, T. R. Knutson, R. J. Stouffer, and F. Zeng, 2003: Twentieth-century temperature and precipitation trends in ensemble climate simulations including natural and anthropogenic forcing. *J. Geophys. Res.,* **108,** 4798, doi:10.1029/2003JD003812.

Cess, R. D., and Coauthors, 1990: Intercomparison and interpretation of climate feedback processes in 19 atmospheric general circulation models. *J. Geophys. Res.,* **95,** 16 601–16 615.

Colman, R., 2003: A comparison of climate feedbacks in general circulation models. *Climate Dyn.,* **20,** 865–873.

Cook, J., and E. J. Highwood, 2004: Climate response to absorbing aerosols in an intermediate general circulation model. *Quart. J. Roy. Meteor.,* **130,** 175–191.

Cubash, U., and Coauthors, 2001: Projections of future climate change. *Climate Change 2001: The Scientific Basis,* J. T. Houghton et al., Eds., Cambridge University Press, 525–582.

Feichter, J., E. Roeckner, U. Lohmann, and B. Liepert, 2004: Nonlinear aspects of the climate response to greenhouse gas and aerosol forcing. *J. Climate,* **17,** 2384–2398.

Forest, C. E., P. Stone, A. Sokolov, M. Allen, and M. Webster, 2002: Quantifying uncertainties in climate system properties with the use of recent climate observation. *Science,* **295,** 113–117.

——, ——, and A. P. Sokolov, 2006: Estimated PDFs of climate system properties including natural and anthropogenic forcings. *Geophys. Res. Lett.,* **33,** L01709, doi:10.1029/2005GL023977.

Forster, P., M. Blackburn, R. Glover, and K. Shine, 2000: An examination of climate sensitivity for idealized climate change experiments in an intermediate general circulation model. *Climate Dyn.,* **16,** 833–849.

Gregory, J. M., and Coauthors, 2004: A new method for diagnosing radiative forcing and climate sensitivity. *Geophys. Res. Lett.,* **31,** L03205, doi:10.1029/2003GL018747.

Hansen, J., G. Russel, D. Rind, P. Stone, A. Lacis, S. Lebedeff, R. Ruedy, and L. Travis, 1983: Efficient three dimensional global models for climate studies: Models I and II. *Mon. Wea. Rev.,* **111,** 609–662.

——, M. Sato, and R. Ruedy, 1997: Radiative forcing and climate response. *J. Geophys. Res.,* **102,** 6831–6864.

——, and Coauthors, 2005: Efficacy of climate forcings. *J. Geophys. Res.,* **110,** D18104, doi:10.1029/2005JD005776.

Joshi, M., K. Shine, M. Ponater, N. Stuber, R. Sause, and L. Li, 2003: A comparison of climate response to different radiative forcings in three general circulation model: Towards an improved metric of climate change. *Climate Dyn.,* **20,** 846–854.

Meehl, G. A., W. M. Washington, C. Ammann, J. M. Arblaster, T. M. L. Wigley, and C. Tebaldi, 2004: Combinations of natural and anthropogenic forcings and twentieth century climate. *J. Climate,* **17,** 3721–3727.

Meleshko, V. P., V. M. Kattsov, P. V. Sporyshev, S. V. Vavulin, and V. A. Govorkova, 2000: Climate system reaction to anthropogenic forcing: Water vapour, clouds and radiation interaction. *Russ. Meteor. Hydrol.,* **2,** 22–45.

Mickley, L. J., D. J. Jacob, B. D. Field, and D. Rind, 2004: Climate response to the increase in tropospheric ozone since preindustrial times: A comparison between ozone and equivalent CO2 forcings. *J. Geophys. Res.*, **109,** D05106, doi:10.1029/2003JD003653.

Murphy, J. M., D. M. H. Sexton, D. N. Barnett, G. S. Jones, M. J. Webb, M. Collins, and D. A. Stainfirth, 2004: Quantification of modeling uncertainties in a large ensemble of climate change simulations. *Nature,* **430,** 768–772.

Penner, J. E., S. Y. Zhang, and C. C. Chuang, 2003: Soot and smoke may not warm climate. *J. Geophys. Res.,* **108,** 4657, doi:10.1029/2003JD003409.

Ramaswamy, V., and C.-T. Chen, 1997: Liner additivity of climate response for combined albedo and greenhouse perturbations. *Geophys. Res. Lett.,* **24,** 567–570.

Roberts, D. L., and A. Jones, 2004: Climate sensitivity to black carbon aerosol from fossil fuel combustion. *J. Geophys. Res.,* **109,** D16202, doi:10.1029/2004JD004676.

Senior, C. A., and J. F. B. Mitchell, 1993: Carbon dioxide and climate: The impact of cloud parameterization. *J. Climate,* **6,** 393–418.

Shine, K. P., J. Cook, E. J. Highwood, and M. M. Joshi, 2003: An alternative to radiative forcing for estimating the relative importance of climate change mechanisms. *Geophys. Res. Lett.,* **30,** 2047, doi:10.1029/2003GL018141.

Sokolov, A., and P. Stone, 1998: A flexible climate model for use in integrated assessments. *Climate Dyn.,* **14,** 291–303.

Stott, P. A., S. F. B. Tett, G. S. Jones, M. R. Allen, J. F. B. Mitchell, and G. J. Jenkins, 2000: External control of 20th century

temperature by natural and anthropogenic forcings. *Science,* **290,** 2133–2137.

Stuber, N., M. Ponater, and R. Sausen, 2005: Why radiative forcing might fail as a predictor of climate change. *Climate Dyn.,* **24,** 497–510.

Wang, C., R. G. Prinn, and A. Sokolov, 1998: A global interactive chemistry and climate model: Formulation and testing. *J. Geophys. Res.,* **103,** 3399–3418.

Washington, W. M., and G. A. Meehl, 1993: Greenhouse sensitivity experiments with penetrative cumulus convection and tropical cirrus albedo effects. *Climate Dyn.,* **8,** 211–223.

Webster, M., and Coauthors, 2003: Uncertainty analysis of climate change and policy response. *Climatic Change,* **61,** 295–320.

Wetherald, R. T., and S. Manabe, 1988: Cloud feedback processes in a general circulation model. *J. Atmos. Sci.,* **45,** 1397–1415.

Yao, M.-S., and A. D. Del Genio, 1999: Effects of cloud parameterization on the simulation of climate changes in the GISS GCM. *J. Climate,* **12,** 761–779.